Velocity-selective optical pumping in four-wave mixing

Geoffrey L. Rogers
200 East 16 Street, New York, New York 10003

P. R. Berman
Physics Department, University of Michigan, Ann Arbor, Michigan 48109
(Received 29 November 1993)

The effects of velocity-selective optical pumping in nearly degenerate four-wave mixing are studied using a model in which the radiation fields interact with "three-level" atoms in the Λ configuration. The conditions under which it is possible to observe resonances characterized by an effective ground-state width are explored. It is shown that saturation of the system by optical pumping can lead to the disappearance of these narrow resonances in some limiting cases.

PACS number(s): 32.80.Bx, 42.65.Hw

I. INTRODUCTION

Optical pumping among the ground-state sublevels in a multilevel atom can significantly affect spectroscopic line shapes. Ground-state optical pumping occurs in weak fields if the interaction time of the atoms with the fields is much longer than the inverse optical pumping rates. In this article, we examine the weak-field saturation effects induced by optical pumping of the ground state in nearly degenerate four-wave mixing (ND4WM) (see Fig. 1). In particular, we determine under what conditions narrow resonances (having a width determined by some effective ground-state relaxation rate) can appear in the ND4WM line shapes. The narrow resonances can be exploited in the construction of optical filters or for locking two laser frequencies together. Moreover they can be used to monitor ground-state relaxation processes. One of the goals of this article is to establish the background for a future planned article in which we will attempt to explain the experimental results of Liu and Steel [1]. In their experiment, Liu and Steel studied the effect of collisions on the narrow resonance in ND4WM.

In a typical experiment involving ND4WM, one measures the intensity of the four-wave-mixing signal as a function of the detuning between two of the incident fields. When the fields drive transitions between multilevel ground- and excited-state manifolds, the ND4WM profile generally consists of narrow and broad resonances characterized by the ground- and excited-state relaxation rates, respectively [2,3]. The ground-state relaxation rate is determined by both the optical pumping rate Γ_p and the transit time $\tau=\gamma_t^{-1}$ that an atom spends in the field interaction region. If the saturation parameter $S=\Gamma_p\tau \gg 1$, optical pumping effects cannot be neglected [4].

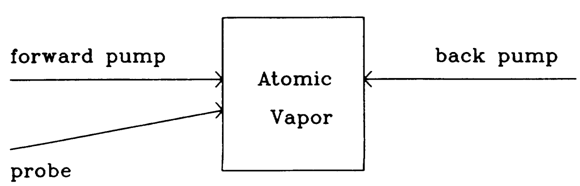

FIG. 1. Configuration of the input beams in nearly degenerate four-wave mixing. The output, or the phase-conjugate beam, propagates in the direction opposite to that of the probe.

Optical pumping creates population imbalance in the atomic ground states through the cycle of excitation and spontaneous emission. Since the laser linewidth and excited-state width may be much narrower than the atomic thermal distribution, this process can be velocity selective. When the laser detuning falls within the Doppler profile of the distribution, those atoms whose velocity brings them into resonance are more strongly coupled to the field and thus undergo optical pumping more rapidly than those atoms that are not in resonance, resulting in a velocity-dependent redistribution of population among ground-state sublevels. Thus velocity-selective optical pumping (VSOP) can create ground-state velocity distributions in a multilevel atom very different from a Maxwellian thermal distribution. This distortion can involve shifting population between magnetic sublevels, giving rise to a velocity-dependent magnetic polarization to zeroth order in the applied fields [5], and the shifting of population between the ground-state hyperfine levels, giving rise to a velocity-dependent zeroth order hyperfine population difference [6]. This distortion in the ground-state populations can have a significant influence on measured line shapes in different types of spectroscopy. The effect of VSOP has been analyzed in two-photon spectroscopy [6], polarization spectroscopy [7], and saturation spectroscopy [8], and VSOP has been utilized in Doppler-free spectroscopy [9]. In addition, VSOP has been utilized to study collisional effects [10]. Our work builds on these earlier studies and demonstrates the importance of VSOP in ND4WM.

It will be seen that, in certain cases, optical pumping can result in the disappearance of the narrow resonance. The disappearance of the narrow resonance in the ND4WM signal of "closed" two-level systems (systems in which the sum of ground- plus excited-state populations is conserved, except possibly for an overall decay rate) is

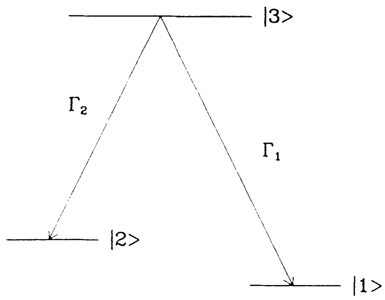

FIG. 2. Three-level atom in the Λ configuration. The incident fields drive both the 1-3 and 2-3 transitions.

already well documented [2,3]. In some respects, the disappearance of the narrow resonance for the multilevel ground-state system can be interpreted in terms of a "closing by saturation." A major objective of our work is to examine in detail this process of closing by saturation, using as a prototype atomic system the three-level Λ scheme shown in Fig. 2.

The article is organized as follows. In Sec. II we solve the density-matrix equations of motion for a three-level atom to obtain the ND4WM signal. In doing so we find the solutions for the third-order optical coherences, which are responsible for the phase-conjugate emission, and also solutions for the unmodulated part of the ground-state populations, which show the effects of optical pumping. We consider the ND4WM signal for several saturations, and show that when the intensity of the back pump is sufficiently weak, the system is able to close by saturation, and the narrow resonance disappears. In Sec. III, we analyze the conditions under which the atom is able to close by saturation. We suggest several situations where this effect may be demonstrated, and we outline an interpretation of a recent experiment which will be more fully analyzed in a forthcoming article.

II. FOUR-WAVE MIXING WITH VELOCITY-SELECTIVE OPTICAL PUMPING

Many of the important features of closing by saturation in the ND4WM line shape can be demonstrated in a "three-level atom," in the Λ configuration shown in Fig. 2. Three fields are incident on the atomic medium: a forward and a backward pump, respectively, and a probe, as shown in Fig. 1. The frequency spacing between levels 2 and 1, ω_{21}, is less than the Doppler width ku (k is the field propagation constant, and u is the most probable atomic speed), such that each field drives both the $1\rightarrow 3$ and $2\rightarrow 3$ transitions. On the other hand, ω_{21} is much greater than the rate at which optical pumping transfers population between states 1 and 2, allowing one to neglect any coherence between states 1 and 2, i.e., the density-matrix element ρ_{12} can be set equal to zero. The atoms are initially in a thermal distribution and the Doppler width of the distribution is much greater than the excited-state decay rate.

A. Density-matrix equations of motion

To calculate the ND4WM signal, it is necessary to solve the density-matrix equations of motion. The density matrix, considered as a function of classical position and momentum variables, evolves as

$$\frac{d\rho}{dt}=\frac{1}{i\hbar}[H,\rho]+\dot{\rho}|_{\text{relaxation}}+\Lambda , \tag{2.1a}$$

with a Hamiltonian $H=H_0+V$, where H_0 is the atomic Hamiltonian given by

$$H_0=\hbar\begin{bmatrix}\omega_3 & 0 & 0\\ 0 & \omega_2 & 0\\ 0 & 0 & \omega_1\end{bmatrix} , \tag{2.1b}$$

and V is the interaction Hamiltonian given by

$$V=-\mathbf{d}\cdot\mathbf{E}$$

or

$$V=-\begin{bmatrix}0 & \mathbf{d}_{32}\cdot\mathbf{E} & \mathbf{d}_{31}\cdot\mathbf{E}\\ \mathbf{d}_{23}\cdot\mathbf{E} & 0 & 0\\ \mathbf{d}_{13}\cdot\mathbf{E} & 0 & 0\end{bmatrix} , \tag{2.1c}$$

where $\mathbf{d}$ is the dipole operator, and $\mathbf{E}$ is the total electric field

$$\mathbf{E}=\tfrac{1}{2}\sum_{m=f,p,b}\mathbf{E}_m\exp[i(\mathbf{k}_m\cdot\mathbf{r}-\Omega_m t)]+\text{c.c.} \tag{2.2}$$

The subscripts f,p,b refer to the forward pump, the probe, and the backward pump, respectively. The forward and backward pumps travel in opposite directions, ($\mathbf{k}_b=-\mathbf{k}_f=-k_f\hat{z}$), and the probe makes a small angle with respect to the forward pump, $\mathbf{k}_p=k_p\cos\theta\hat{z}+k_p\sin\theta\hat{x}$, where $\hat{z}$ and $\hat{x}$ are unit vectors in the z and x directions, respectively, and $\theta\ll 1$. In this three-level model, the vectorial nature of the fields and the dipole matrix elements are irrelevant; each of the fields couples both $1\rightarrow 3$ and $2\rightarrow 3$. In all cases, the fields are weak, i.e., the Rabi frequency associated with each field is much less than the spontaneous emission rate. The forward pump and probe are taken to have equal field strength, and the strength of the backward pump is variable. The two pumps have the same frequency, and the probe is slightly detuned from the pumps: $\Omega_f=\Omega_b\equiv\Omega$ and $\Omega_p=\Omega+\delta$.

The relaxation terms in the density-matrix equations are specified as

$$\dot{\rho}_{33}|_{\text{rel}}=-(\Gamma+\gamma_t)\rho_{33} , \tag{2.3a}$$

$$\dot{\rho}_{22}|_{\text{rel}}=\Gamma_2\rho_{33}-\gamma_t\rho_{22} , \tag{2.3b}$$

$$\dot{\rho}_{11}|_{\text{rel}}=\Gamma_1\rho_{33}-\gamma_t\rho_{11} , \tag{2.3c}$$

$$\dot{\rho}_{23}|_{\text{rel}}=-(\Gamma/2+\gamma_t)\rho_{23} , \tag{2.3d}$$

$$\dot{\rho}_{13}|_{\text{rel}}=-(\Gamma/2+\gamma_t)\rho_{13} , \tag{2.3e}$$

where Γ is the total spontaneous emission rate from level 3, Γ_1 and Γ_2 are the spontaneous emission rates from level 3 to levels 1 and 2, respectively, and γ_t is the inverse transit time.

The pumping matrix is

$$\Lambda = \begin{bmatrix} 0 & 0 & 0 \\ 0 & \lambda/2 & 0 \\ 0 & 0 & \lambda/2 \end{bmatrix} , \tag{2.4}$$

where the pumping rate is $\lambda = \gamma_t W$ and W is a Maxwellian distribution,

$$W(v) = (\pi u)^{-3/2} \exp(-v^2/u^2) . \tag{2.5}$$

This pumping matrix leads to equal populations in states 1 and 2 in the absence of applied fields [11].

Expanding Eq. (2.1a) and assuming $|(\Omega_m - \omega_{ij})/(\Omega_m + \omega_{ij})| \ll 1$, one obtains

$$\dot{\rho}_{33} = i \sum_{\alpha=f,p,b} (\chi_2^\alpha e^{i(\mathbf{k}_\alpha \cdot \mathbf{r} - \Omega_\alpha t)} \rho_{23} + \chi_1^\alpha e^{i(\mathbf{k}_\alpha \cdot \mathbf{r} - \Omega_\alpha t)} \rho_{13}) + \text{c.c.} - (\Gamma + \gamma_t) \rho_{33} , \tag{2.6a}$$

$$\dot{\rho}_{22} = -i \sum_{\alpha=f,p,b} \chi_2^\alpha e^{i(\mathbf{k}_\alpha \cdot \mathbf{r} - \Omega_\alpha t)} \rho_{23} + \text{c.c.} + \Gamma_2 \rho_{33} - \gamma_t \rho_{22} + \lambda/2 , \tag{2.6b}$$

$$\dot{\rho}_{11} = -i \sum_{\alpha=f,p,b} \chi_1^\alpha e^{i(\mathbf{k}_\alpha \cdot \mathbf{r} - \Omega_\alpha t)} \rho_{13} + \text{c.c.} + \Gamma_1 \rho_{33} - \gamma_t \rho_{11} + \lambda/2 , \tag{2.6c}$$

$$\dot{\rho}_{32} = -(i\omega_{32} + \Gamma/2 + \gamma_t) \rho_{32} + i \sum_{\alpha=f,p,b} \chi_2^\alpha e^{i(\mathbf{k}_\alpha \cdot \mathbf{r} - \Omega_\alpha t)} (\rho_{22} - \rho_{33}) , \tag{2.6d}$$

$$\dot{\rho}_{31} = -(i\omega_{31} + \Gamma/2 + \gamma_t) \rho_{31} + i \sum_{\alpha=f,p,b} \chi_1^\alpha e^{i(\mathbf{k}_\alpha \cdot \mathbf{r} - \Omega_\alpha t)} (\rho_{11} - \rho_{33}) , \tag{2.6e}$$

$$\rho_{ij} = \rho_{ji}^* ,$$

where the Rabi frequency is defined as

$$\chi_i^\alpha = \frac{\mathbf{d}_{3i} \cdot \mathbf{E}_\alpha}{2\hbar}, \quad i = 1,2 , \tag{2.7}$$

and $\omega_{ij} = \omega_i - \omega_j$ is the transition frequency between levels i and j. The derivative is the total derivative $\dot{\rho}_{ij} = (\partial/\partial t + \mathbf{v} \cdot \nabla) \rho_{ij}$.

One solves these equations in the steady state to third order in the field amplitudes for the coherences ρ_{31} and ρ_{32} by an expansion in the field modulation starting with zeroth-order ground-state populations. As a result of interference of the different fields, the ground-state populations are spatially modulated; these modulations are referred to as the population "gratings." The term "zeroth order" refers to that part of the population that is *not* spatially modulated. As a result of optical pumping by each field acting separately, the zeroth-order populations need not be zeroth order in the applied fields. Rather, they are zeroth order in the modulation, and are the same as the spatially averaged populations. The terms "zeroth-order population," "unmodulated part of the population," and "spatially averaged population" all refer to the same quantity.

Using standard procedures for solving the density-matrix equations, one first obtains solutions for the populations and uses these solutions in the expression for the relevant component of the optical coherence. The populations are obtained as a Fourier expansion in the modulation, but only the lowest-order terms contribute significantly. Successive terms in the expansion decrease in magnitude as powers of the ratio of the optical pumping rate to the effective grating decay rate. Only terms of zeroth and first order are significant.

The effective grating decay rate is determined by thermal washout: the time it takes a thermal atom to traverse the spatial grating. The spatial period of the lowest-order grating formed by the forward pump and the probe is $2\pi/|\mathbf{k}_f - \mathbf{k}_p|$, and the most probable speed of a thermal atom is u. Therefore a thermal atom traverses the grating in a time $(|\mathbf{k}_f - \mathbf{k}_p| u)^{-1}$ so the gratings wash out due to thermal motion over times of order $(|\mathbf{k}_f - \mathbf{k}_p| u)^{-1}$. The effective grating decay rate resulting from thermal motion is therefore $|\mathbf{k}_f - \mathbf{k}_p| u \equiv \gamma_{\text{grat}}$.

The optical pumping rate $\Gamma_p \approx |\chi|^2 \Gamma$ is the rate at which the combined action of the fields and spontaneous emission transfers population between states 1 and 2. The rate that the lowest-order grating is created is Γ_p and the rate that it decays is γ_{grat}, so one expects the lowest-order grating amplitude to be of order $\Gamma_p/\gamma_{\text{grat}}$ and the higher-order grating amplitudes to decrease in magnitude as powers of this ratio. In the problems considered here, the field strength is small enough that

$$\Gamma_p \ll |\mathbf{k}_f - \mathbf{k}_p| u , \tag{2.8}$$

so one can drop the higher-order terms from the Fourier expansion.

The first-order coherences are obtained from Eqs. (2.6d) and (2.6e) by factoring out the rapidly oscillating part

$$\rho_{ij}^{(1)} = \sum_{\beta=f,p,b} \rho_{ij}^\beta e^{i(\mathbf{k}_\beta \cdot \mathbf{r} - \Omega_\beta t)} . \tag{2.9}$$

Using the orthogonality of the exponential functions and the fact that in the steady state $\dot{\rho}_{ij}^\beta = 0$, one obtains

$$\rho_{32}^\beta = \frac{i \chi_2^\beta \rho_{22}^{(0)}}{-i(\Delta_2^\beta - \mathbf{k}_\beta \cdot \mathbf{v}) + \Gamma/2} \tag{2.10a}$$

and

$$\rho_{31}^\beta = \frac{i \chi_1^\beta \rho_{11}^{(0)}}{-i(\Delta_1^\beta - \mathbf{k}_\beta \cdot \mathbf{v}) + \Gamma/2} , \tag{2.10b}$$

where the detuning $\Delta_i^\beta = \Omega_\beta - \omega_{3i}$, $\rho_{11}^{(0)}$, and $\rho_{22}^{(0)}$ are the (as yet unknown) zeroth-order ground-state sublevel populations, and $\Gamma \gg \gamma_t$.

The second-order populations are spatially modulated due to interference between the different waves. One expands the second-order population as a sum of modulated terms,

$$\rho_{nn}^{(2)} = \sum_{\alpha,\beta=f,p,b} \rho_{nn}^{\alpha\beta} \exp i(\mathbf{k}_{\alpha\beta} \cdot \mathbf{r} - \Omega_{\alpha\beta} t) , \tag{2.11}$$

where $\mathbf{k}_{\alpha\beta} = \mathbf{k}_\alpha - \mathbf{k}_\beta$, $\Omega_{\alpha\beta} = \Omega_\alpha - \Omega_\beta$, and $\dot{\rho}_{nn}^{\alpha\beta} = 0$ in the steady state. The $\rho_{nn}^{\alpha\beta}$ with $\alpha \neq \beta$ are the population grating amplitudes. The zeroth order, or unmodulated terms, are obtained from Eq. (2.11) by summing with $\alpha=\beta$,

$$\rho_{nn}^{(0)}=\sum_{\alpha}\rho_{nn}^{\alpha\alpha} . \tag{2.12}$$

Using the orthogonality of the exponential functions, and using Eqs. (2.6a) and (2.10), one obtains steady-state solutions for the excited-state grating amplitudes given by

$$\rho_{33}^{\alpha\beta}=\frac{1}{-i(\Omega_{\alpha\beta}-\mathbf{k}_{\alpha\beta}\cdot\mathbf{v})+\Gamma}\left[\chi_2^{\alpha}\chi_2^{\beta*}\left[\frac{1}{i(\Delta_2^{\beta}-\mathbf{k}_{\beta}\cdot\mathbf{v})+\Gamma/2}+\frac{1}{-i(\Delta_2^{\alpha}-\mathbf{k}_{\alpha}\cdot\mathbf{v})+\Gamma/2}\right]\rho_{22}^{(0)}\right.$$
$$\left.+\chi_1^{\alpha}\chi_1^{\beta*}\left[\frac{1}{i(\Delta_1^{\beta}-\mathbf{k}_{\beta}\cdot\mathbf{v})+\Gamma/2}+\frac{1}{-i(\Delta_1^{\alpha}-\mathbf{k}_{\alpha}\cdot\mathbf{v})+\Gamma/2}\right]\rho_{11}^{(0)}\right] . \tag{2.13}$$

Using Eqs. (2.6b) and (2.6c) for the ground-state populations, Eq. (2.13) for the excited-state population, and Eqs. (2.10) for the coherences, one obtains an equation for the time evolution of the ground-state populations:

$$\frac{d}{dt}\rho_{ii}=\lambda/2-\sum_{j=1,2}\sum_{\alpha\beta}\chi_j^{\alpha}\chi_j^{\beta}\exp i(\mathbf{k}_{\alpha\beta}\cdot\mathbf{r}-\Omega_{\alpha\beta}t)$$
$$\times\left[\left[\delta_{ij}-\frac{\Gamma_i}{-i(\Omega_{\alpha\beta}-\mathbf{k}_{\alpha\beta}\cdot\mathbf{v})+\Gamma}\right]\right.$$
$$\left.\times\left[\frac{1}{i(\Delta_j^{\beta}-\mathbf{k}_{\beta}\cdot\mathbf{v})+\Gamma/2}+\frac{1}{-i(\Delta_j^{\alpha}-\mathbf{k}_{\alpha}\cdot\mathbf{v})+\Gamma/2}\right]+\gamma_t\delta_{ij}\right]\rho_{jj}^{(0)} , \tag{2.14}$$

where $i=1,2$, and

$$\delta_{ij}=\begin{cases}1, & i=j\\ 0, & i\neq j .\end{cases} \tag{2.15}$$

When Eq. (2.11) is substituted into Eq. (2.14), the resulting equations can be solved for $\rho_{nn}^{\alpha\beta}$ in the steady state. The ground-state grating amplitudes ($\alpha\neq\beta$) are given by

$$\rho_{22}^{\alpha\beta}=\frac{1}{-i(\Omega_{\alpha\beta}-\mathbf{k}_{\alpha\beta}\cdot\mathbf{v})+\gamma_t}$$
$$\times\left[\chi_2^{\alpha}\chi_2^{\beta*}\left[-1+\frac{\Gamma_2}{-i(\Omega_{\alpha\beta}-\mathbf{k}_{\alpha\beta}\cdot\mathbf{v})+\Gamma}\right]\left[\frac{1}{i(\Delta_2^{\beta}-\mathbf{k}_{\beta}\cdot\mathbf{v})+\Gamma/2}+\frac{1}{-i(\Delta_2^{\alpha}-\mathbf{k}_{\alpha}\cdot\mathbf{v})+\Gamma/2}\right]\rho_{22}^{(0)}\right.$$
$$\left.+\chi_1^{\alpha}\chi_1^{\beta*}\left[\frac{\Gamma_2}{-i(\Omega_{\alpha\beta}-\mathbf{k}_{\alpha\beta}\cdot\mathbf{v})+\Gamma}\right]\left[\frac{1}{i(\Delta_1^{\beta}-\mathbf{k}_{\beta}\cdot\mathbf{v})+\Gamma/2}+\frac{1}{-i(\Delta_1^{\alpha}-\mathbf{k}_{\alpha}\cdot\mathbf{v})+\Gamma/2}\right]\rho_{11}^{(0)}\right] . \tag{2.16}$$

One obtains a similar expression for $\rho_{11}^{\alpha\beta}$ with the interchange of indices $1\leftrightarrow2$ in Eq. (2.16). In this expression, one sees that, indeed, the lowest-order grating amplitude is of order $\Gamma_p/\gamma_{\text{grat}}$. The solution of Eq. (2.14) for $\rho_{11}^{(0)}$ and $\rho_{22}^{(0)}$ is given in Sec. II C below.

Using Eqs. (2.6d) and (2.11), one obtains an expression for the third-order coherences,

$$\dot{\rho}_{3i}^{(3)}=-(i\omega_{3i}+\Gamma/2)\rho_{3i}^{(3)}$$
$$+i\sum_{\alpha\beta\gamma}\chi_i^{\gamma}(\rho_{ii}^{\alpha\beta}-\rho_{33}^{\alpha\beta})\exp[i(\mathbf{k}_{\gamma}+\mathbf{k}_{\alpha}-\mathbf{k}_{\beta})\cdot\mathbf{r}$$
$$-i(\Omega_{\gamma}+\Omega_{\alpha}-\Omega_{\beta})t] , \tag{2.17}$$

with $i=1,2$. Of all the terms in the sum in Eq. (2.17), only two contribute to the phase-conjugate wave: those for which $\mathbf{k}_{\gamma}+\mathbf{k}_{\alpha}-\mathbf{k}_{\beta}=-\mathbf{k}_p$, with $(\gamma,\alpha,\beta)=(f,b,p)$ and $(\gamma,\alpha,\beta)=(b,f,p)$. The third-order coherence is decomposed into a sum of modulated terms,

$$\rho_{3i}^{(3)}=\sum_{\alpha\beta\gamma}\rho_{3i}^{\alpha\beta\gamma}\exp[i(\mathbf{k}_{\gamma}+\mathbf{k}_{\alpha}-\mathbf{k}_{\beta})\cdot\mathbf{r}$$
$$-i(\Omega_{\gamma}+\Omega_{\alpha}-\Omega_{\beta})t] ,$$

and the relevant component is given by

$$\rho_{3i}^{(3)}(-\mathbf{k}_p,\Omega-\delta)=\frac{i\chi_i^{b}(\rho_{ii}^{fp}-\rho_{33}^{fp})}{-i(\Delta_i-\delta+\mathbf{k}_p\cdot\mathbf{v})+\Gamma/2}$$
$$+[\text{same with } f\leftrightarrow b] , \tag{2.18}$$

where $\Delta_i=\Omega-\omega_{3i}$, $-\mathbf{k}_p$ is the wave vector, and $\Omega-\delta$ the frequency of the phase-conjugate wave. The first term corresponds to the back pump scattering off a grating formed by the forward pump and probe and the second term corresponds to the forward pump scattering off a grating formed by the back pump and probe. The second term in Eq. (2.18) does not contribute appreciably to the phase-conjugate wave. The grating size of the back pump-probe grating is of order $1/2k$ so the grating effective decay rate (inverse of the time it takes a thermal atom to traverse the grating) is $2ku$. This is much larger than the population decay rates; the back pump-probe grating is washed out over time intervals of interest in this problem, due to the thermal motion of the atoms, and can be ignored. Only the first term in Eq. (2.18) is considered in the following discussion.

The relevant difference grating is

$$\rho_{22}^{fp}-\rho_{33}^{fp}=-\chi_2^f\chi_2^{p*}\rho_{22}^{(0)}\mathcal{L}_2\left[\frac{1}{i(\delta-\kappa v_x)+\gamma_t}\left[1-\frac{\Gamma_2}{i(\delta-\kappa v_x)+\Gamma}\right]+\frac{1}{i(\delta-\kappa v_x)+\Gamma}\right]$$
$$-\chi_1^f\chi_1^{p*}\rho_{11}^{(0)}\mathcal{L}_1\left[\frac{1}{i(\delta-\kappa v_x)+\Gamma}-\frac{1}{i(\delta-\kappa v_x)+\gamma_t}\frac{\Gamma_2}{i(\delta-\kappa v_x)+\Gamma}\right], \tag{2.19}$$

where

$$\mathcal{L}_i=\frac{1}{i(\Delta_i+\delta-kv_z-\kappa v_x)+\Gamma/2}+\frac{1}{-i(\Delta_i-kv_z)+\Gamma/2} \tag{2.20}$$

and $k\equiv|\mathbf{k}_f|,\kappa\approx|\mathbf{k}_f-\mathbf{k}_p|\approx k\theta$, and v_z, v_x are the z,x components of the atomic velocity. One obtains a similar expression for $\rho_{11}^{fp}-\rho_{33}^{fp}$ with the interchange of the indices $1\leftrightarrow2$ in Eq. (2.19).

The terms in square brackets can be simplified by expanding in partial fractions to get

$$\rho_{22}^{fp}-\rho_{33}^{fp}=-\chi_2^f\chi_2^{p*}\rho_{22}^{(0)}\mathcal{L}_2\left[\frac{\alpha_1}{i(\delta-\kappa v_x)+\gamma_t}+\frac{1+\alpha_2}{i(\delta-\kappa v_x)+\Gamma}\right]$$
$$+\chi_1^f\chi_1^{p*}\rho_{11}^{(0)}\mathcal{L}_1\left[\frac{-\alpha_2}{i(\delta-\kappa v_x)+\gamma_t}+\frac{1+\alpha_2}{i(\delta-\kappa v_x)+\Gamma}\right], \tag{2.21}$$

where the branching ratio $\alpha_i=\Gamma_i/\Gamma$ and $\Gamma\gg\gamma_t$. Again, an interchange of indices $1\leftrightarrow2$ will give $\rho_{11}^{fp}-\rho_{33}^{fp}$. The first term in each of the square brackets is responsible for the narrow resonances in the ND4WM line shape. In the limit that $\alpha_2\to1$ and $\alpha_1\to0$, the system is a closed two-level system (between levels 2 and 3) and one sees in Eq. (2.21) that the narrow resonance associated with this transition disappears. The fact that the $2\to3$ transition is open allows the ground-state grating to decay at a much slower rate; there is a "residual" ground-state grating.

One notes that the narrow resonance disappears if the coefficient of $[i(\delta-\kappa v_x)+\gamma_t]^{-1}$ is zero, or if

$$\Gamma_1\chi_2^f\chi_2^{p*}\rho_{22}^{(0)}\mathcal{L}_2=\Gamma_2\chi_1^f\chi_1^{p*}\rho_{11}^{(0)}\mathcal{L}_1\ ,$$

which can occur if $\rho_{11}^{(0)}$ and $\rho_{22}^{(0)}$ are distorted in an appropriate way through optical pumping.

B. Nonlinear polarization

The ND4WM signal is proportional to $|P(-\mathbf{k}_p,\Omega-\delta)|^2$, where

$$P(-\mathbf{k}_p,\Omega-\delta)=\int[d_{32}^*\rho_{32}^{(3)}(-\mathbf{k}_p,\Omega-\delta)+d_{31}^*\rho_{31}^{(3)}(-\mathbf{k}_p,\Omega-\delta)]d^3v$$

or

$$P(-\mathbf{k}_p,\Omega-\delta)=-i\frac{E_fE_bE_p^*}{8\hbar^3}\int(\{|d_{32}|^4\mathcal{L}_{22}[\alpha_1L(\gamma_t)+(1+\alpha_2)L(\Gamma)]$$
$$+|d_{31}|^2|d_{32}|^2\mathcal{L}_{12}[-\alpha_1L(\gamma_t)+(1+\alpha_1)L(\Gamma)]\}\rho_{22}^{(0)}$$
$$+\{|d_{32}|^2|d_{31}|^2\mathcal{L}_{21}[-\alpha_2L(\gamma_t)+(1+\alpha_2)L(\Gamma)]$$
$$+|d_{31}|^4\mathcal{L}_{11}[\alpha_2L(\gamma_t)+(1+\alpha_1)L(\Gamma)]\}\rho_{11}^{(0)})d^3v\ , \tag{2.22}$$

where

$$\mathcal{L}_{ij}=\frac{1}{-i(\Delta_i-\delta+kv_z+\kappa v_x)+\Gamma/2}\left[\frac{1}{i(\Delta_j+\delta-kv_z-\kappa v_x)+\Gamma/2}+\frac{1}{-i(\Delta_j-kv_z)+\Gamma/2}\right] \tag{2.23}$$

and

$$L(\gamma)=\frac{1}{i(\delta-\kappa v_x)+\gamma}\ . \tag{2.24}$$

Using

$$|d_{32}|^2 \equiv \mu_2 |d|^2, \quad |d_{31}|^2 \equiv \mu_1 |d|^2 , \tag{2.25}$$

where d is a "reduced matrix element," one can write Eq. (2.22) as

$$P(-\mathbf{k}_p, \Omega-\delta) = -i \frac{E_f E_b E_p^* |d|^4}{8\hbar^3} \times \int (\{\mu_2^2 \mathcal{L}_{22}[\alpha_1 L(\gamma_t) + (1+\alpha_2) L(\Gamma)] + \mu_1\mu_2 \mathcal{L}_{12}[-\alpha_1 L(\gamma_t) + (1+\alpha_1) L(\Gamma)]\}\rho_{22}^{(0)} + \{\mu_2\mu_1 \mathcal{L}_{21}[-\alpha_2 L(\gamma_t) + (1+\alpha_2) L(\Gamma) + \mu_1^2 \mathcal{L}_{11}[\alpha_2 L(\gamma_t) + (1+\alpha_1) L(\Gamma)]\}\rho_{11}^{(0)}) d^3 v . \tag{2.26}$$

This expression can be expressed in a more compact form by defining

$$a_{ij} = \mu_i \mu_j \alpha_{3-j} (-1)^{i+j}, \quad b_{ij} = \mu_i \mu_j (1+\alpha_i) , \tag{2.27}$$

so that

$$P(-\mathbf{k}_p, \Omega-\delta) = -i \frac{E_f E_b E_p^* |d|^4}{8\hbar^3} \sum_{ij} \int [a_{ij} L(\gamma_t) + b_{ij} L(\Gamma)] \mathcal{L}_{ij} \rho_{jj}^{(0)} d^3 v . \tag{2.28}$$

To evaluate this expression for the polarization, one must first determine the zeroth order sublevel populations.

C. Zeroth-order sublevel populations

In this section expressions for the zeroth order, or unmodulated part of the ground-state sublevel populations, are obtained. The sublevel populations are affected by optical pumping, and the amount of optical pumping depends on the saturation. The saturation parameter, $S = \Gamma_p / \gamma_t$ is defined as the ratio of the resonant atomic excitation rate to the inverse transit time.

If the system is unsaturated ($S \ll 1$), there is no significant optical pumping, and $\rho_{11}^{(0)} = \rho_{22}^{(0)} = \frac{1}{2} W(\mathbf{v})$, where $W(\mathbf{v})$ is given by Eq. (2.5). In this case, the integrals in Eq. (2.28) can be expressed in terms of plasma dispersion functions [12].

The system is saturated if $S \gg 1$. In this case there is significant optical pumping, and the zeroth-order ground-state sublevel populations are distorted.

To determine the zeroth-order or unmodulated part of the sublevel populations, one obtains a set of coupled rate equations for $\rho_{11}^{(0)}$ and $\rho_{22}^{(0)}$ from Eq. (2.14), the ground-state equation of motion, and Eq. (2.12):

$$\dot{\rho}_{22}^{(0)} = -\left[\gamma_t + \frac{\Gamma_1}{\Gamma} R_2\right] \rho_{22}^{(0)} + \frac{\Gamma_2}{\Gamma} R_1 \rho_{11}^{(0)} + \lambda/2 \tag{2.29a}$$

and

$$\dot{\rho}_{11}^{(0)} = -\left[\gamma_1 + \frac{\Gamma_2}{\Gamma} R_1\right] \rho_{11}^{(0)} + \frac{\Gamma_1}{\Gamma} R_2 \rho_{22}^{(0)} + \lambda/2 , \tag{2.29b}$$

where the total excitation rate out of level i is

$$R_i = R_i^f + R_i^p + R_i^b , \tag{2.30}$$

and

$$R_i^f = \frac{|\chi_i^f|^2 \Gamma}{(\Delta_i - k v_z)^2 + (\Gamma/2)^2} , \tag{2.31a}$$

$$R_i^p = \frac{|\chi_i^p|^2 \Gamma}{(\Delta_i + \delta - k v_z)^2 + (\Gamma/2)^2} , \tag{2.31b}$$

$$R_i^b = \frac{|\chi_i^b|^2 \Gamma}{(\Delta_i + k v_z)^2 + (\Gamma/2)^2} . \tag{2.31c}$$

In the steady state, Eqs. (2.29) can be solved to yield (using $\lambda = \gamma_t W$)

$$\rho_{22}^{(0)} = \frac{(\alpha_2 R_1 + \gamma_t/2) W}{\alpha_2 R_1 + \alpha_1 R_2 + \gamma_t} \tag{2.32a}$$

and

$$\rho_{11}^{(0)} = \frac{(\alpha_1 R_2 + \gamma_t/2) W}{\alpha_1 R_2 + \alpha_2 R_1 + \gamma_t} , \tag{2.32b}$$

where $\alpha_i = \Gamma_i / \Gamma$. It is noted that the zeroth-order population is conserved: $\rho_{11}^{(0)} + \rho_{22}^{(0)} = W$.

Equations (2.32) can be expressed in terms of the saturation parameter S if Eq. (2.25) is used to set $|\chi_i^m|^2 = \mu_i |\chi^m|^2$, where $\chi^m = d E_m / (2\hbar)$. The forward pump and probe are taken to have equal field strength, and the field strength of the back probe is variable: $|\chi^f| = |\chi^p| \equiv |\chi|$ and $|\chi^b|^2 = \beta |\chi|^2$, where $0 < \beta \le 1$. One can then write Eqs. (2.32) as

$$\rho_{22}^{(0)} = \frac{[\tilde{R}_1 + 1/(2S)] W}{\tilde{R}_1 + \tilde{R}_2 + 1/S} , \tag{2.33a}$$

$$\rho_{11}^{(0)} = \frac{[\tilde{R}_2 + 1/(2S)] W}{\tilde{R}_1 + \tilde{R}_2 + 1/S} , \tag{2.33b}$$

where

$$\tilde{R}_i(v_z) = \mu_i \alpha_{3-i} \left[\frac{1}{[(\Delta_i - k v_z)/\Gamma]^2 + \frac{1}{4}} + \frac{1}{[(\Delta_i + \delta - k v_z)/\Gamma]^2 + \frac{1}{4}} + \frac{\beta}{[(\Delta_i + k v_z)/\Gamma]^2 + \frac{1}{4}} \right] , \tag{2.34}$$

$$S=\Gamma_p/\gamma_t \ , \tag{2.35}$$

and

$$\Gamma_p=\frac{|\chi|^2}{\Gamma} \ . \tag{2.36}$$

Since the different velocity components do not couple to each other, one may factor out the v_x, v_y, and v_z dependencies of the populations

$$\rho_{ii}^{(0)}(\mathbf{v})=n_i(v_z)W_x(v_x)W_y(v_y) \ , \tag{2.37}$$

where $W_i(v_i)=(\sqrt{\pi}u)^{-1}[-v_i^2/u^2]$ is the one-dimensional thermal distribution, and

$$n_2(v_z)=\frac{[\tilde{R}_1(v_z)+1/(2S)]W_z(v_z)}{\tilde{R}_1(v_z)+\tilde{R}_2(v_z)+1/S} \ , \tag{2.38a}$$

$$n_1(v_z)=\frac{[\tilde{R}_2(v_z)+1/(2S)]W_z(v_z)}{\tilde{R}_1(v_z)+\tilde{R}_2(v_z)+1/S} \ . \tag{2.38b}$$

Figures 3(a)–3(c) show n_1 and n_2 as a function of velocity for several values of S and a full strength back pump ($\beta=1$). In these plots, the width of the thermal distribution is $ku=100\Gamma$, the probe detuning is $\delta=0$, the ground-state splitting is $\omega_{21}=150\Gamma$, the detuning of the pump from the $2\rightarrow3$ transition is $\Delta_2=10\Gamma$, and $\alpha_i=\mu_i=\frac{1}{2}$, $i=1,2$.

One sees that for increasing transit times (increasing saturation), the populations become more distorted. The holes in the n_2 distribution and the peaks in the n_1 distribution are at $kv=\pm10\Gamma$, corresponding to those atoms that are Doppler shifted into resonance with radiation driving the $2\rightarrow3$ transition, and have been pumped out

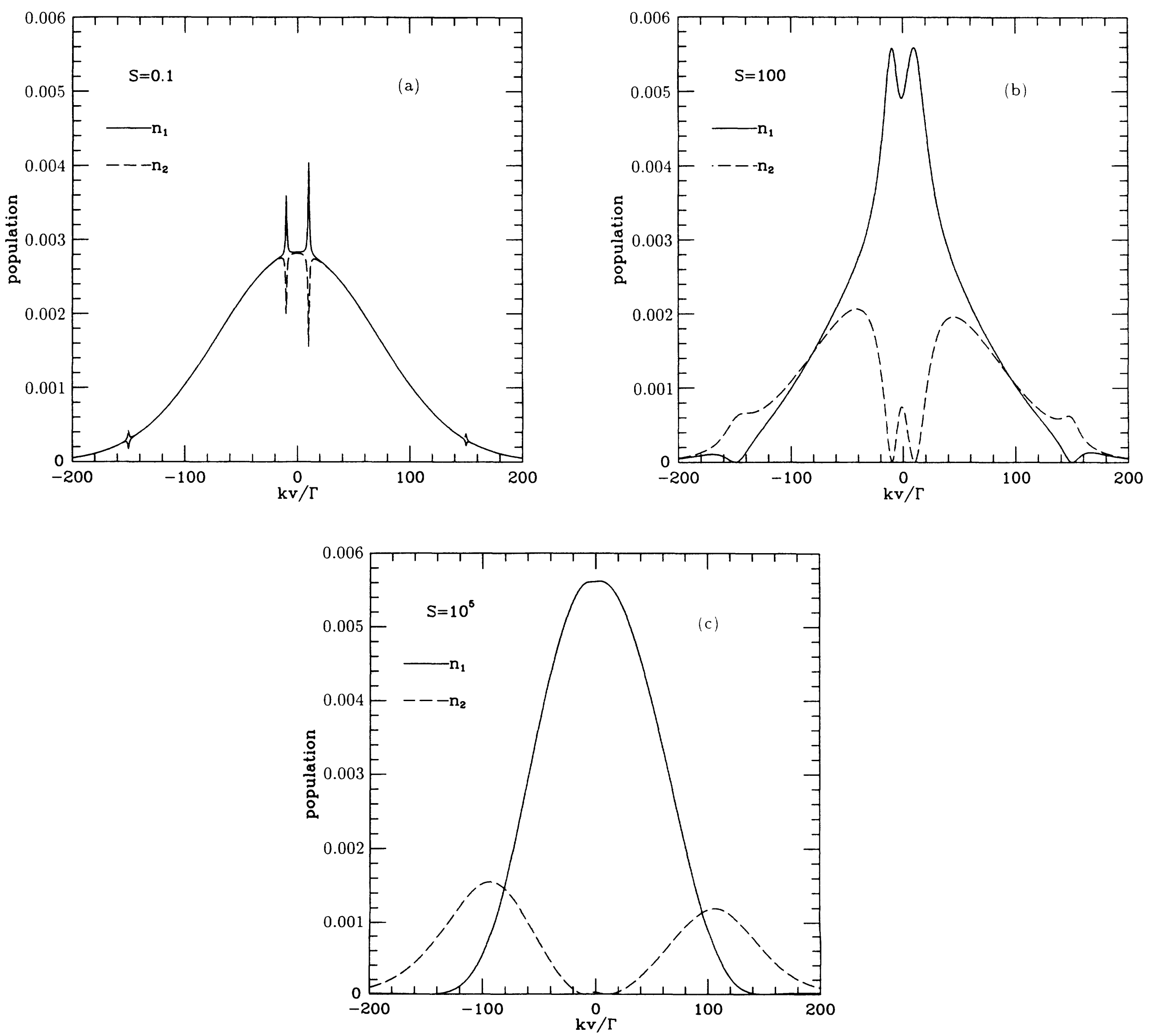

FIG. 3. Ground-state population densities as a function of kv/Γ for $ku/\Gamma=100$, $\delta/\Gamma=0$, $\Delta_2/\Gamma=10$, $\Delta_1/\Gamma=-150$, and $\beta=1$. (a) $S=0.1$. (b) $S=100$. (c) $S=10^5$.

of level 2 into level 1. The forward pump and the back pump are resonant with different velocity classes since they are traveling in opposite directions, as can be seen in the expressions for R_i^f and R_i^b, Eqs. (2.31). The atoms at $kv=+10\Gamma$ are resonant with the forward pump and probe and the atoms at $kv=-10\Gamma$ are resonant with the back pump. The small peaks in the wings of the n_2 distribution and holes in the n_1 distribution correspond to those atoms Doppler shifted into resonance with radiation driving the $1\rightarrow 3$ transition and have been pumped from level 1 to level 2. These peaks occur at $kv=-160\Gamma$ for the forward pump and probe and at $kv=+160\Gamma$ for the back pump. The asymmetry in these curves is due to the fact that the forward pump and the probe are resonant with the same atoms (when $\delta=0$), so that those atoms get excited at twice the rate of those that are resonant with the back pump.

For larger transit times (larger S), the resonances in the distributions become "saturation broadened." In the fully saturated system ($\gamma_t\rightarrow 0, S\rightarrow\infty$), Fig. 3(c), the distributions are independent of the field intensity, as can be seen from Eqs. (2.38). In each velocity class, the sublevel populations have been altered in such a way that the rate that zeroth-order or *spatially averaged* population is transferred from level 2 to level 1 by excitation and spontaneous emission is equal to the rate that *spatially averaged* population is transferred from level 1 to level 2. One can define this condition as "full saturation of the *population*." This condition is directly related to the disappearance of the narrow resonance from the ND4WM line shape, as is shown below.

D. Four-wave mixing signal

One can now evaluate the polarization and obtain the ND4WM signal. Using Eq. (2.37) for the $\rho_{ii}^{(0)}$, the polarization, Eq. (2.28), can be expressed as

$$P(-\mathbf{k}_p,\Omega-\delta)=-\frac{E_f E_b E_p^*|d|^4}{8\hbar^3\kappa u}\sum_{ij}\left[a_{ij}Z\left[\frac{i\gamma_t-\delta}{\kappa u}\right]+b_{ij}Z\left[\frac{i\Gamma-\delta}{\kappa u}\right]\right]\langle\mathcal{L}_{ij}\rangle\ , \tag{2.39}$$

where a_{ij},b_{ij} are given in Eq. (2.27), $Z(\mu)$ is the plasma dispersion function [12] defined by

$$Z(\mu)=-\frac{1}{\sqrt{\pi}}\int_{-\infty}^{+\infty}dx\frac{e^{-x^2}}{\mu\pm x},\quad \mathrm{Im}(\mu)>0\ , \tag{2.40}$$

and

$$\langle\mathcal{L}_{ij}\rangle=\int_{-\infty}^{+\infty}\frac{1}{-i(\Delta_i-\delta+kv_z)+\Gamma/2}\left[\frac{1}{i(\Delta_j+\delta-kv_z)+\Gamma/2}+\frac{1}{-i(\Delta_j-kv_z)+\Gamma/2}\right]n_j(v_z)dv_z\ , \tag{2.41}$$

where we have used the fact (consistent with the calculations done here) that $(\kappa u)^2\ll(\Delta_i)^2$. Figure 4(a) shows a plot of the ND4WM signal [modulus squared of Eq. (2.39)] as a function of δ/Γ, for an unsaturated system, $S=0.1$. The back pump has the same intensity as the forward pump ($\beta=1$). The detunings, the thermal width, and the branching ratios are the same as previously: $\Delta_1=-150\Gamma$, $\Delta_2=10\Gamma$, $ku=100\Gamma$, $\alpha_i=\mu_i=\frac{1}{2}$, $i=1,2$.

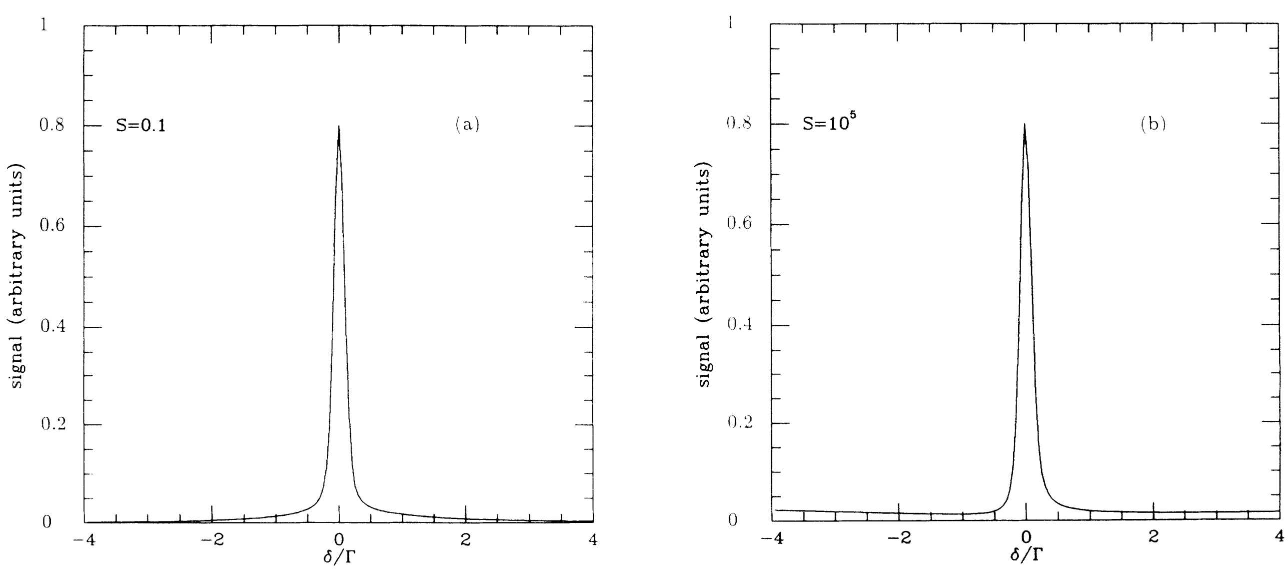

FIG. 4. ND4WM signal in arbitrary units as a function of δ/Γ for $ku/\Gamma=100$, $\Delta_2/\Gamma=10$, $\Delta_1/\Gamma=-150$, $\beta=1$, and $\kappa u/\Gamma=0.1$. (a) $S=0.1$. (b) $S=10^5$. The shape of the signal is independent of S; however, in absolute terms, the signal strength in (b) is 10^{-6} times smaller than that in (a).

The angle between the pump and the probe is $\theta = 10^{-3}$ rad, so $\kappa u = \Gamma/10$.

Figure 4(a) shows a sharp peak (the narrow resonance) on top of a broad pedestal at $\delta = 0$. The pedestal has a half width at half maximum (HWHM) of Γ. The width of the sharp peak is due to the residual Doppler broadening (or the grating dephasing rate) and is of order $\Gamma/10$.

Plots of the ND4WM signal for larger values of S are nearly identical to Fig. 4(a), except that the height of the peak decreases with increasing saturation. The atoms that contribute most strongly to the signal are those that are resonant with the forward pump and probe and those that are resonant with the back pump. As shown in the figures for the populations, Figs. 3(a)–3(c), the population of the resonant atoms decreases as the saturation increases. This is reflected in the fact that the signal peak decreases with increasing saturation, such that the peak of the fully saturated signal ($S \rightarrow \infty$) is 10^{-6} that of the unsaturated signal. The signal strength decreases due to a decrease in resonant population, but the shape of the signal, i.e., the height and width of the narrow peak compared to the broad pedestal, does not change for reasons to be discussed below. Figure 4(b) is a plot of the signal from a fully saturated system. The value of $S = 10^5$ is chosen to illustrate the response of a fully saturated system. In practice, however, it is difficult to satisfy inequality (2.8) for the parameters of Figs. 4(b) and 5, since values $\Gamma/\gamma_t > 10^5$ are implied.

When the intensity of the back probe is decreased, however, the narrow resonance does disappear in the fully saturated system. This is demonstrated in Figs. 5(a)–5(c), which show the ND4WM signal for decreasing

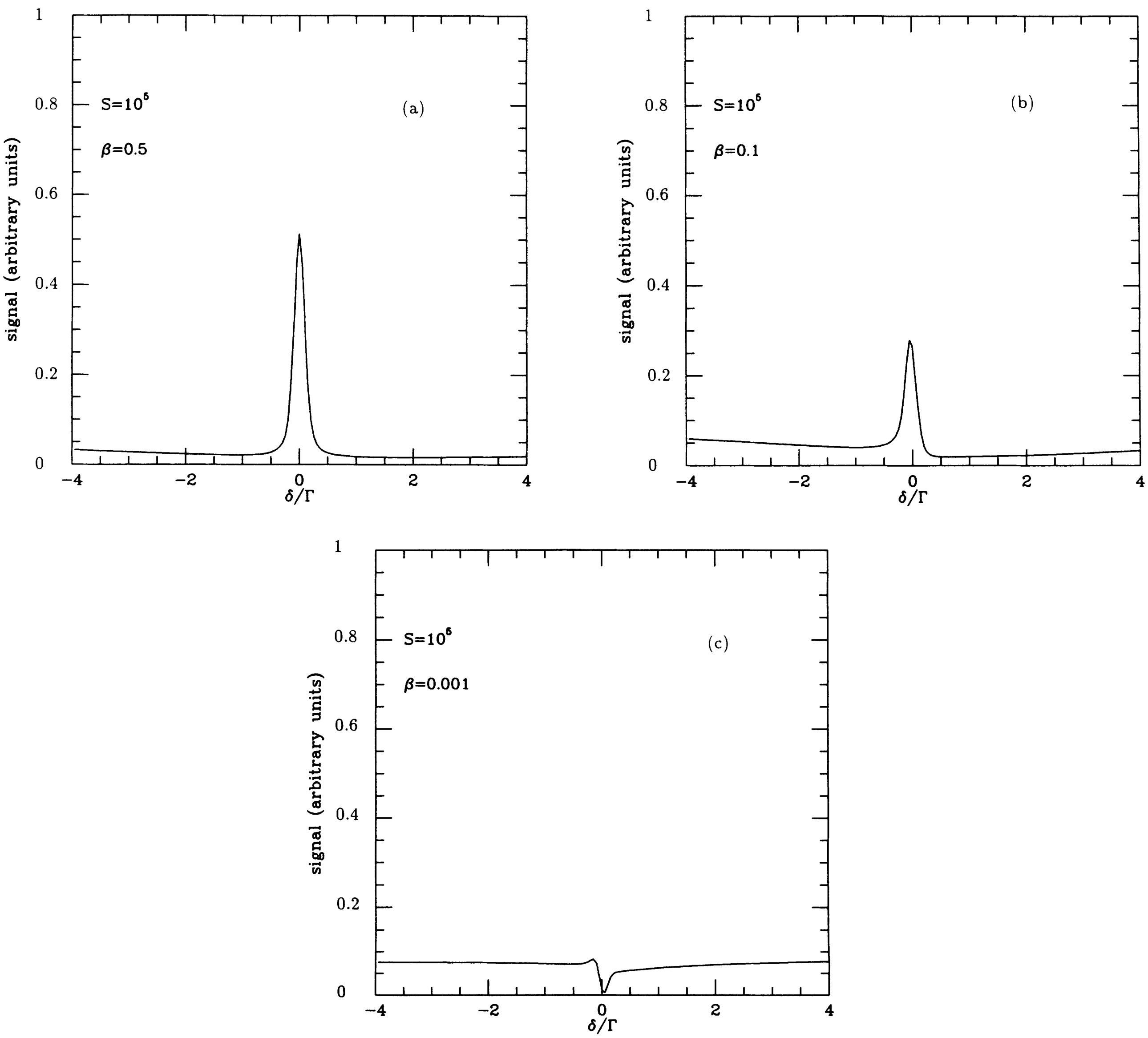

FIG. 5. ND4WM signal in arbitrary units as a function of δ/Γ in the large saturation limit for $ku/\Gamma = 100$, $\Delta_2/\Gamma = 10$, $\Delta_1/\Gamma = -150$, $\kappa u/\Gamma = 0.1$, and $S = 10^5$. (a) $\beta = 0.5$. (b) $\beta = 0.1$. (c) $\beta = 0.001$. In each of these plots, the vertical scale is the same as that used in Fig. 4(b).

values of β. The same absolute scale is used in each of the figures, which is the same scale used in Fig. 4(b). The parameters are the same as those in Fig. 4(b), with the exception of β. In this case, the signal is the intensity of the phase-conjugate wave divided by the intensity of the back pump.

III. CLOSING BY SATURATION

In the following, the reason for this disappearance of the narrow resonance from the ND4WM line shape is discussed. First, a general condition for the disappearance of the narrow resonance is obtained, and then it is shown that this condition is satisfied when the back pump is weak ($\beta \ll 1$). It is shown that fulfillment of the condition is related to the degree of saturation the system undergoes, and is therefore called closing by saturation.

It is shown below that the narrow resonance disappears if

$$\rho_{22}^{fp}+\frac{\Gamma_2}{\Gamma}\rho_{33}^{fp}=0\ , \tag{3.1}$$

where ρ_{ii}^{fp} is the level i grating amplitude formed by the forward pump and probe, given by Eqs. (2.13) and (2.16), respectively, and Γ_2/Γ is the fraction of atoms in the excited state that decays to level 2. If Eq. (3.1) is satisfied, then the level 2 (and level 1) grating is "filled in" due to spontaneous emission at the same rate that the excited-state grating decays; there is no "residual" ground-state grating. The depth of modulation and the phase of the excited-state grating is such that the portion of the excited-state grating that decays to level 2 just "fills" the level 2 grating. Thus the level 2 grating decays at the spontaneous emission rate, and the narrow resonance does not appear in the ND4WM line shape. If Eq. (3.1) holds then there is a similar relation for ρ_{11}^{fp}. Equation (3.1) can be satisfied only when $S\rightarrow\infty$. As indicated earlier, when $S\rightarrow\infty$ the spatially averaged *populations* are always saturated. In the following, it is shown that there is a distinction between saturation of the spatially averaged *populations* and saturation of the *gratings.* It is saturation of the gratings that is implied in Eq. (3.1).

The *populations* are fully saturated if the spatial average of the number of atoms per unit time that are transferred from level 2 to level 1 by excitation and spontaneous emission is equal to the number of atoms per unit time that are transferred from level 1 to level 2, such that the spatial average of the net population transfer rate is zero. The population of a velocity class in level 2 that is close to resonance is decreased by optical pumping, while the population of the same velocity class in level 1 is far from resonance and will be increased by optical pumping. This is clearly shown in Figs. 3(a)–3(c). If $S\rightarrow\infty$, the resonant population of level 2 has decreased and the same velocity class in level 1 has increased to such an extent that the *spatial average* of the net population transfer rate between the sublevels is zero. Saturation of the spatially averaged populations always occurs when $S\rightarrow\infty$.

If the spatial average of the net population transfer rate between ground-state sublevels is zero, it directly follows that the spatially averaged rate at which population is excited from level 2 to level 3 is equal to the spatially averaged rate that level 2 is repopulated by spontaneous emission from level 3. This condition defines fully saturated *populations.*

Full saturation of the *gratings* is defined as that condition for which the rate that atoms are excited into the level 3 grating from level 2 is equal to the rate that the level 2 grating is repopulated due to spontaneous emission from the level 3 grating. Saturation of the *populations* is defined in terms of the *spatially averaged* populations, while saturation of the *gratings* is defined in terms of the *modulated* part of the populations.

In the following it is demonstrated that Eq. (3.1) is indeed satisfied and thus the narrow resonance disappears from the ND4WM spectrum when the gratings are fully saturated. It follows from Eq. (2.18) and Eq. (2.21) that the narrow resonance disappears if the term multiplying $[i(\delta-\kappa v_x)+\gamma_t]^{-1}$ in Eq. (2.21) for $\rho_{22}^{fp}-\rho_{33}^{fp}$ vanishes, i.e., if

$$\Gamma_1\chi_2^f\chi_2^{p*}\mathcal{L}_2\rho_{22}^{(0)}=\Gamma_2\chi_1^f\chi_1^{p*}\mathcal{L}_1\rho_{11}^{(0)}\ . \tag{3.2}$$

On the other hand, it follows immediately from Eqs. (2.13) and (2.16) that

$$\rho_{22}^{fp}+\frac{\Gamma_2}{\Gamma}\rho_{33}^{fp}=\frac{1/\Gamma}{i(\delta-\kappa v_x)+\gamma_t}[-\Gamma_1\chi_2^f\chi_2^{p*}\mathcal{L}_2\rho_{22}^{(0)}+\Gamma_2\chi_1^f\chi_1^{p*}\mathcal{L}_1\rho_{11}^{(0)}]\ . \tag{3.3}$$

Clearly, if Eq. (3.2) holds so does Eq. (3.1), confirming our hypothesis concerning the filling in of the gratings.

It is interesting to compare the conditions for saturation of the zeroth-order (unmodulated) populations and saturation of the gratings. Using Eqs. (2.29) one finds that the condition for saturation of the zeroth-order populations is

$$-\Gamma_1R_2\rho_{22}^{(0)}+\Gamma_2R_1\rho_{11}^{(0)}=0\ . \tag{3.4}$$

It follows from Eqs. (2.33) that Eq. (3.4) is satisfied in the limit of strong saturation by *any* of the incident fields ($R_i\gg\gamma_t$), where R_i is given by Eq. (2.30). On the other hand, Eq. (3.2), the condition for saturation of the grating, is generally *not* satisfied even if $R_i\gg\gamma_t$. The zeroth-order populations do not adjust themselves to allow for saturation of the gratings. To examine this in more detail, we consider the limit when $|\delta-\kappa u|\ll\Gamma$ and $|\chi_i^p|=|\chi_i^f|$, such that

$$\chi_i^f\chi_i^{p*}\mathcal{L}_i\approx\tfrac{1}{2}(R_i^f+R_i^p)\equiv\tfrac{1}{2}R_i^{fp}\ ,$$

where R_i^f and R_i^p are the excitation rates from level i to level 3 due to the forward pump and the probe, respectively, given by Eqs. (2.31), and $\frac{1}{2}R_i^{fp}\rho_{ii}^{(0)}$ is the rate that population is excited into the level 3 *gratings* from level i. One can write Eq. (3.2) as

$$-\Gamma_1R_2^{fp}\rho_{22}^{(0)}+\Gamma_2R_1^{fp}\rho_{11}^{(0)}=0\ . \tag{3.5}$$

Comparing Eq. (3.4) with Eq. (3.5), one can see that the grating will saturate along with the zeroth-order populations if $R_i^{fp}\approx R_i$ or $R_i^{fp}\propto R_i$. Several examples for which these conditions hold are given below.

The effect of the back pump differs principally from that of the forward pump in that it is resonant with a different velocity class. If the velocity selectivity of the excitation rates is removed, then the back pump does not affect the zeroth-order velocity distributions and the *gratings* saturate when the *populations* saturate. One way this can occur is if the atomic thermal width is very small ($ku \ll \Gamma$). Another way to remove the velocity selectivity is to have collisions that thermalize the distributions. This situation is treated in a planned future article where the disappearance of the narrow resonance in a ND4WM experiment [1] is explained in terms of this effect.

Finally, if the back pump intensity is much less than the forward pump intensity $\beta \ll 1$, then the effect of the back pump on the zeroth-order populations is significantly reduced. With $\beta \ll 1$, $R_i \approx R_i^{fp}$ and the gratings fully saturate when the populations are fully saturated. This is demonstrated in Figs. 5(a)–5(c). The height of the narrow peak decreases relative to the background as β decreases. Figures 6(a)–6(c) demonstrate the effect of the back pump on the population distributions by showing n_1 and n_2 for a saturated system, for various values of β. The values of the other parameters are the same as those in Figs. 3(a)–3(c). As β decreases, the n_1 and n_2 distributions become approximately independent of β indicating that the back pump has little influence on the sublevel populations for most velocity classes for small values of β.

IV. CONCLUSION

The basic ideas of closing by saturation have been developed here. It has been shown that when the gratings are saturated, there is no "residual" ground-state grating, and the narrow resonance does not appear in the

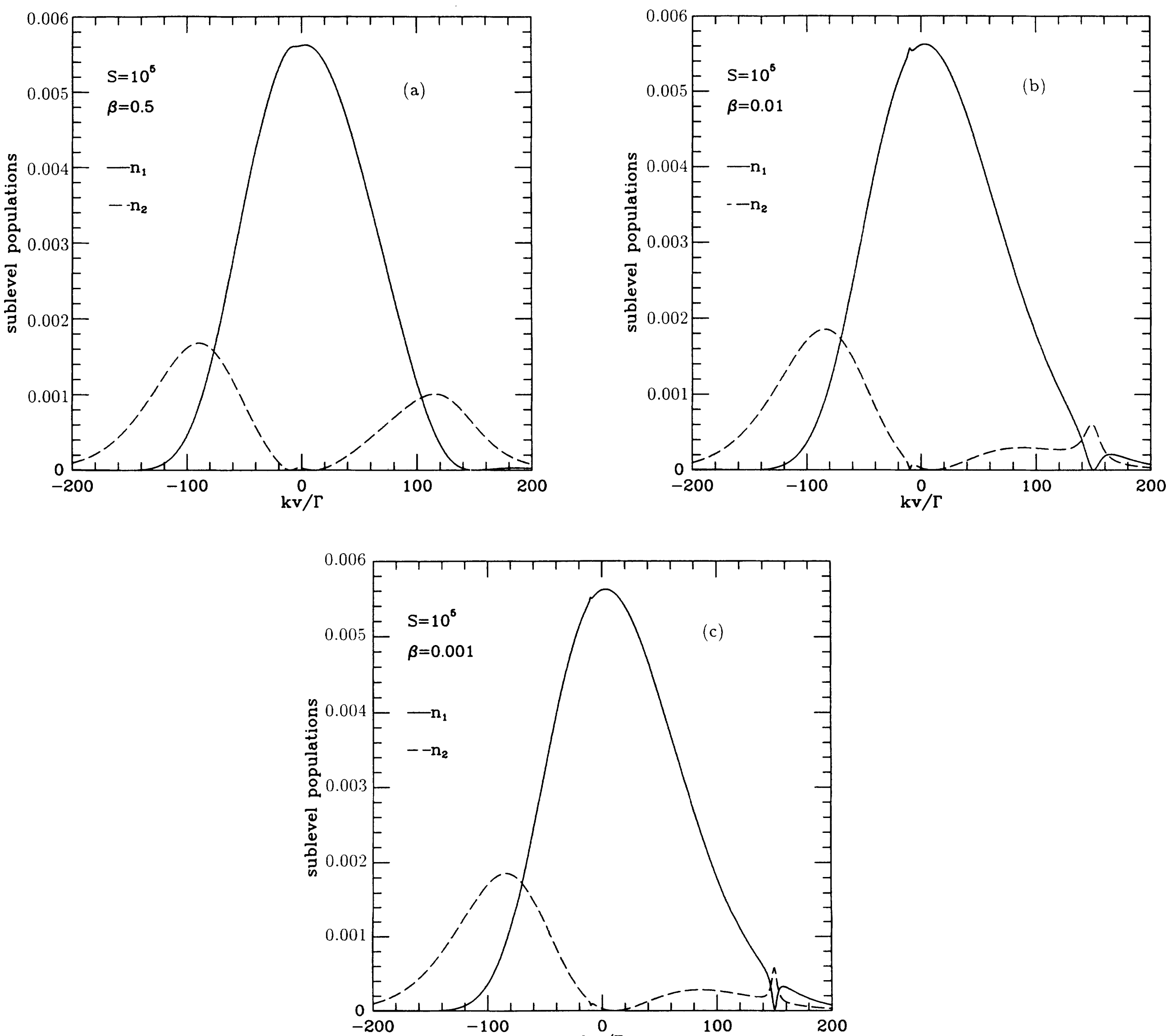

FIG. 6. Ground-state population densities as a function of δ/Γ in the large saturation limit for $ku/\Gamma=100$, $\delta/\Gamma=0$, $\Delta_2/\Gamma=10$, $\Delta_1/\Gamma=-150$, and $S=10^5$. (a) $\beta=0.5$. (b) $\beta=0.1$. (c) $\beta=0.001$.

ND4WM line shape. The connection with a closed two-level system is as follows. In a closed two-level system, in each velocity class, the number of atoms per unit time excited out of the ground state is equal to the number of atoms per unit time repopulating the ground state by spontaneous emission. In such a case there is no residual ground-state grating. In a multilevel atom, this condition must be satisfied by each of the sublevels individually. Moreover, it must be satisfied not only by the spatially averaged populations but by the grating amplitudes as well. In the multilevel atom, this condition can be satisfied only if the populations have been altered by optical pumping. Saturation of the populations and saturation of the gratings both depend critically on the size, in each velocity subclass, of the sublevel populations. The spatially averaged populations always saturate for $S \rightarrow \infty$, but whether the gratings formed by the forward pump and probe saturate in this limit depends on the effect of the back pump. If the back pump influences the population distributions, the gratings do not saturate. Therefore one expects the appearance of the narrow resonance in the ND4WM spectrum in systems where the back pump does influence the sublevel population distributions, and its disappearance in systems in which the back pump does not affect the population distributions.

The qualitative features of the role played by velocity-selective optical pumping are illustrated in the three-level model adopted in this work. This has been confirmed by calculations carried out for the actual level schemes of sodium atoms, using incident fields all having the same polarization [13]. The qualitative features of the line shapes with sodium as the active atom are similar to those for the three-level atoms considered in this work.

The idea of closing by saturation is used in a forthcoming article to interpret a ND4WM experiment [1], where the narrow resonance disappears when the active atoms are immersed in a high-pressure buffer gas. The buffer gas increases the diffusive transit time of the atoms through the interaction region, allowing significant optical pumping to develop, and also destroys the velocity selectivity of the ground-state optical pumping by collisional redistribution. As a result, the back pump does not affect the velocity distributions. Therefore the system is able to close by saturation, and the narrow resonance does not appear.

ACKNOWLEDGMENT

This research is supported by the National Science Foundation through Grants Nos. PHY-9113590 and PHY-9396245.

[1] J. Liu and D. G. Steel, Phys. Rev. A **38**, 4639 (1988).

[2] P. R. Berman, Phys. Rev. A **43**, 1470 (1991).

[3] P. R. Berman, D. G. Steel, G. Khitrova, and J. Liu, Phys. Rev. A **38**, 252 (1988).

[4] R. Walkup, A. Spielfiedel, W. D. Phillips, and D. E. Pritchard, Phys. Rev. A **23**, 1869 (1981).

[5] C. G. Aminoff and M. Pinard, J. Phys. (Paris) **43**, 263 (1982).

[6] J. E. Bjorkholm, P. F. Liao, and A. Wokaun, Phys. Rev. A **26**, 2643 (1982).

[7] W. Gawlik, Phys. Rev. A **34**, 3760 (1986).

[8] D. E. Murnick, M. S. Feld, M. M. Burns, T. U. Kohl, and P. G. Pappas, in *Laser Spectroscopy IV*, edited by H. Walther and K. W. Rothe (Springer, Berlin, 1979), p. 195; Opt. Lett. **5**, 79 (1980).

[9] M. Pinard, C. G. Aminoff, and F. Laloë, Phys. Rev. A **19**, 2366 (1979).

[10] C. G. Aminoff, J. Javanainen, and M. Kaivola, Phys. Rev. A **28**, 722 (1983).

[11] Choosing unequal pumping rates for the two ground-state sublevels does not significantly affect the results, but leads to unequal populations in the absence of applied fields.

[12] B. D. Fried and S. D. Conte, *The Plasma Dispersion Function* (Academic, New York, 1961).

[13] G. L. Rogers, Ph.D. thesis, New York University, 1992.